Geosfera Indonesia
p-ISSN 2598-9723, e-ISSN 2614-8528
available online at : https://jurnal.unej.ac.id/index.php/GEOSI
Vol. 9 No. 2, August 2024, 176-192

https://doi.org/10.19184/geosi.v9i2.45736

Research Article

Identification of Relict Landslide Parts Based on Morphometric Data to Determine Potential Hazard Zones Combined with Surface Morphodynamics

R. Ramlah*, Redo Saputro
Department of Geography, Institut Teknologi PLN, Jakarta, 11750, Indonesia
*Corresponding author, email : ramlah@itpln.ac.id

ARTICLE INFO

Received :
18 January 2024

Revised :
11 July 2024

Accepted :
20 July 2024

Published :
31 July 2024

ABSTRACT

The destruction of houses and facilities by landslide causes deaths. In this context, the level of destruction and subjective description of the characteristics can be examined through landslide parts determination. Therefore, this study aims to determine potential landslide hazard zone and houses potentially affected. Global Navigation Satellite System (GNSS) and unmanned aerial vehicle (UAV) are morphometric surveys combined with surface morphodynamics to show potential hazard zones of landslide parts. Meanwhile, Data Elevation Model (DEM) is used to delineate relict landslide and the concept is verified by field observation and orthophoto. Morphometric measurements are collected at each slope gradient by GNSS and surface morphodynamics are investigated on the entire relict landslide area by direct observation and orthophoto data. The combination of morphometric and morphodynamic data describes hazard zone of relict landslide. In addition, the integration of orthophoto and landslide hazard zone data is used to determine potentially affected houses. This study was conducted on landslides 1 and 2 with zone classifications of very high, high, low and very low. The results show that there are different conditions and the most hazardous parts of landslides 1 and 2 are the foot and body, respectively. A total of 75 and 50 houses were potentially affected by landslides 1 and 2, respectively. Identification of hazard zones based on landslide parts determines the boundaries of the area affected. The addition of surface activity processes determines the level of hazard in each of parts, while the combination of morphometric and morphodynamic data shows landslide zone.

Keywords: Landslide; Morphometric; Morphodynamic; Hazard; Houses

INTRODUCTION

Indonesia is a country with a high level of vulnerability to natural disasters, specifically in areas of massive structural complexity (Triatmadja, 2011). Natural disasters such as floods, landslides, and earthquakes, cause loss of life, and property, as well as disruption of the order of events (Setyowati, 2019). Landslide is the most common disaster in the hilly regions of Indonesia. Therefore, the hazard level can be controlled through evaluation and zoning (Shano et al., 2020). Vulnerability, hazard and risk assessment are carried out to evaluate landslide at the regional scale (Feng et al., 2022; He et al., 2024; Pellicani et al., 2017; Nefros et al., 2023; Dotta et al., 2023).

Field surveys using satellite imagery data are employed to identify hazard zone, while field data are obtained through measurement and observation (Soldato et al., 2017; Psomiadis et al., 2020; Yan et al., 2023). Coordinate and elevation data are obtained using Global Navigation Systems (GNSS) mapping tool (Xi et al., 2023; Huang et al., 2023; Wang et al., 2022). High-resolution satellite imagery data LiDAR and InSAR are provided through advancements in remote sensing technology (He et al., 2023 & Amatya et al., 2021), while complete data are produced from field survey and remote sensing (Ghorbanzadeh et al., 2020 & Shan et al., 2023). Landslide zone is identified using Unmanned Aerial Vehicles (UAV) and GNSS (Nikolakopoulus et al., 2023; Kyriou et al., 2022; Garnica-Pena & Alcanata-Ayala., 2021). Meanwhile, remote sensing and mathematical methods in the determination of landslide hazard zone (He et al., 2024 & Li et al., 2020).

To determine hazard zones, rainfall, geomorphological and geological aspects must be used based on the intensity and volume (D'Ippolito et al., 2023 & Rong et al., 2020). According to Alvioli et al. (2018) & Saenkang et al (2022), landslide occurrs due to cutting and vibration. The river at the foot of the slope, the road at the crown and foot, as well as the seepage on the slope triggered landslide (Kinde et al., 2024 & Nanehkaran et al., 2023). The combination of the variables is important due to the complexity of the research area and interaction (Thomas et al., 2023 & Kamal et al., 2023). Landslide hazard identification is determined by house positions and materials (Zhang et al., 2024; Fariz et al., 2023; Shi et al., 2023). This showed the necessity to analyze slope conditions and process activities with the interrelationships.

The Bompon Sub-watershed of Bogowonto Watershed is located within Magelang Regency with areas dominated by steep slopes. The location possesses 39 landslide scars with residential houses (Ramlah et al., 2020). Previous studies assessed the landslide hazard to determine the zone of landslide hazards based on morphological variables (slope and geomorphological processes), climatic variables (rainfall) and slope material. As a new insight, in this study, landslide hazard zone was determined based on morphological and climatic variables (rainfall) as well as slope material including landslide zone and part of landslide. The selection of these variables is based on the consideration of conducting several research on the regional scale. The recurrence events are characterized by bodies and many settlements are found in relict landslide. Therefore, this study aims to determine potential landslide hazard zone as well as houses potentially affected.

METHODS

Study Area

This study was conducted at landslide 1 and 2 sites in Margoyoso Village, Salaman Subdistrict, and Magelang District (Figure 1). The location was in the upstream area and transition zone of Sumbing and Merapi Volcano dominated by steep slopes > 40%. Surface material is clay which is a deposit of old and young Sumbing volcanic ash. Subsurface materials are deposits of Kulonprogo Volacano weathered due to the magma activity of Sumbing Volcano. Intensive weathering causes the material to be particularly thick with a depth of > 30 m. The combination resulted in relict landslide identified in the entire watershed Bompon area (Ramlah et al., 2020).

A total of 2 relict landslides were selected due to surface process activity and the presence of settlements. Meanwhile, new formation was found in landslide 1 showing material movement.

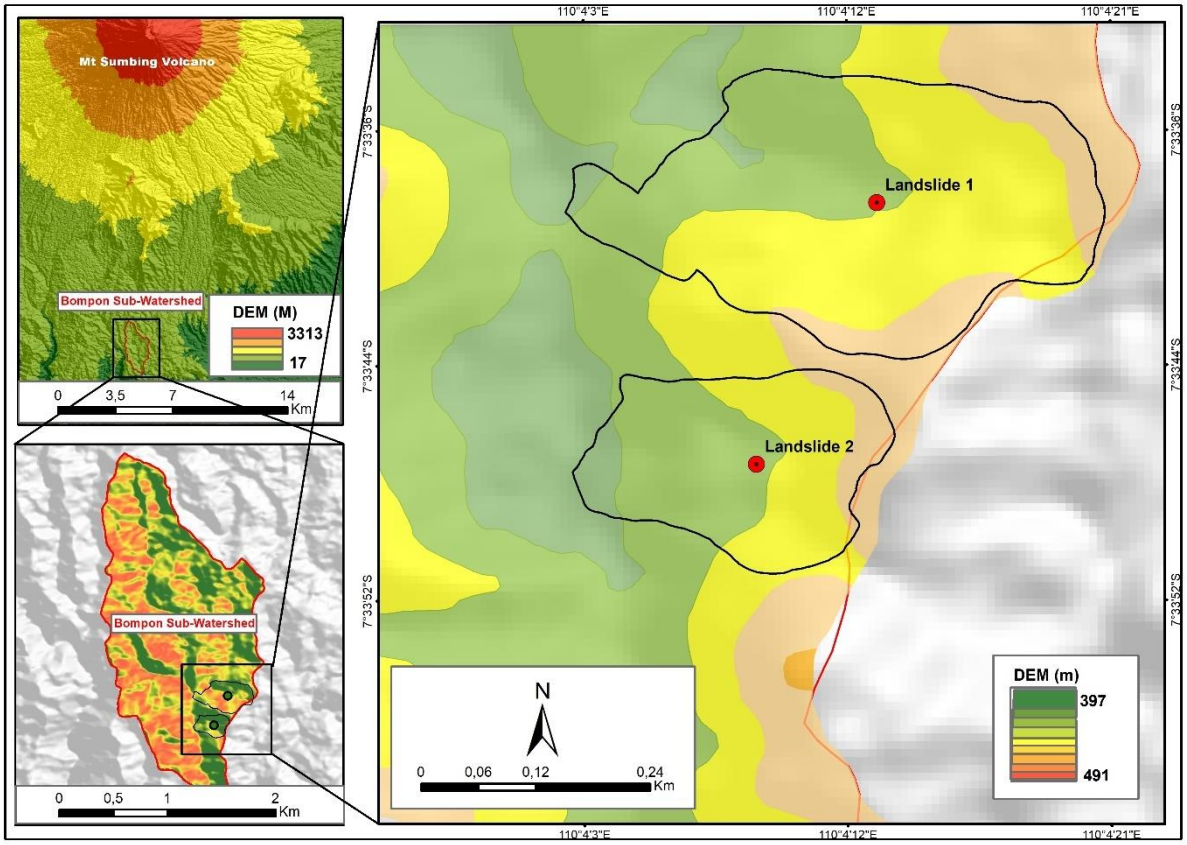

Figure 1. Study Area

Selected Relict Landslide as Object Research

The first step of the research was to identify landslide traces andidentification is based on morphological analysis of the slope using Data Elevation Model (DEM). DEM data was obtained from the Geospatial Information Institution (BIG) https://tanahair.indonesia.go.id/demnas/#/demnas and data from BIG has a resolution accuracy of 8 meters. Subsequently, DEM was analyzed using ArcMap to generate the slope and hillside. The analysis of data produces surface topography describing the shape of the basin (Azmoon et al., 2022). In addition, the basin is identified as a former and relict landslide, as showed in Figure 2.

The second step is to determine landslide site as the object of research. The selection is based on the existence of settlements in the former landslide area and the current ground movement condition. Landslide sites have settlements and the basis of determining the object depends on the presence or absence of ground movement in the scars area. Information was obtained from a rapid survey of the research site and interviews with the local community. The selected landslide scars are those with and without soil movement obtained by comparing the risk of houses affected.

Data Collecting

Morphometric survey is carried out to determine landslide parts before measuring each slope degradation. GNSS with high accuracy is selected due to data required (Xi et al., 2023; Huang et al., 2023; Wang et al., 2022). The subsequent step was to photograph the selected landslide area using the UAV method to identify boundaries and surface morphodynamic activity (Sun et

al., 2024; Jacobs et al., 2017). Houses in the selected landslide site are delineated using an orthophoto, such as Phantom 4 Drone (Li et al., 2020).

In the selected relict landslide, field observation was used to obtain morphodynamic data and human activity. On the track extending from the opposite side of landslide boundary with a width of 100 m, the traverse method used was accomplished by walking zig-zag. During the traverse survey, the information and human activities observed were recorded to support orthophoto data for zone determination (Sun et al., 2024; Jacobs et. al, 2017). The soil moves away within the depletion zone and deposited in accumulation zone (Orgita, 2017).

Data Analysis

The crown, scrap, body, and foot parts of landslide have different characteristics. The crown is the highest part, while scrap is a cliff formed due to soil movement. In addition, the main body is landslide field covered by material and the foot is the flat lower part of the slope (Cooper, 2007). Based on landslide parts characteristics, identification can be carried out by elevation data to identify the higher and the lower parts of landslide.

Morphometric data is analysed by ArcMap to create elevation and contour data. Meanwhile, UAV data is processed by Agisoft Software to create an orthophoto. Data aim to verify and justify the boundary of landslides 1 and 2 (Akcay, 2015). Orthophoto of landslides 1 and 2 are entered into ArcMap and combined with elevation and contour data. Therefore, parts of landslide can be identified and restricted in ArcMap using the information.

Morphodynamic data are plotted according to position in the field with the coordinates obtained by observation. The last analysis is determining landslide potential and house hazard zones. The level of potential hazard zones is based on the characteristics of landslide parts (Gonzales, 2018) and morphodynamic information, as described in Table 1.

Table 1. Classification of Potential Hazard Using Morphodynamic and Morphography Data

Landslide Potentially Hazard Level	Morphodynamic Information	Morphometric Data
Level I (Very High)	New Landslide (smaller size than the previous landslide) Gully Fractures Springs Seepage	Sloping-Extremely Steep
Level II (High)	Fractures Gully Springs Seepage	Sloping-Moderately Slope
Level III (Low)	Rill erosion Springs Seepage	Gently Slope-Flat
Level IV (Very Low)	Dense Vegetation	Gently Slope-Flat

The classification of the slope is based on Van Zuidam, while the measurement and collection of data use high-resolution tools. However, the determination of potential hazard zones is semi-quantitative and guaranteed to be similar due to differences in material and climate conditions.

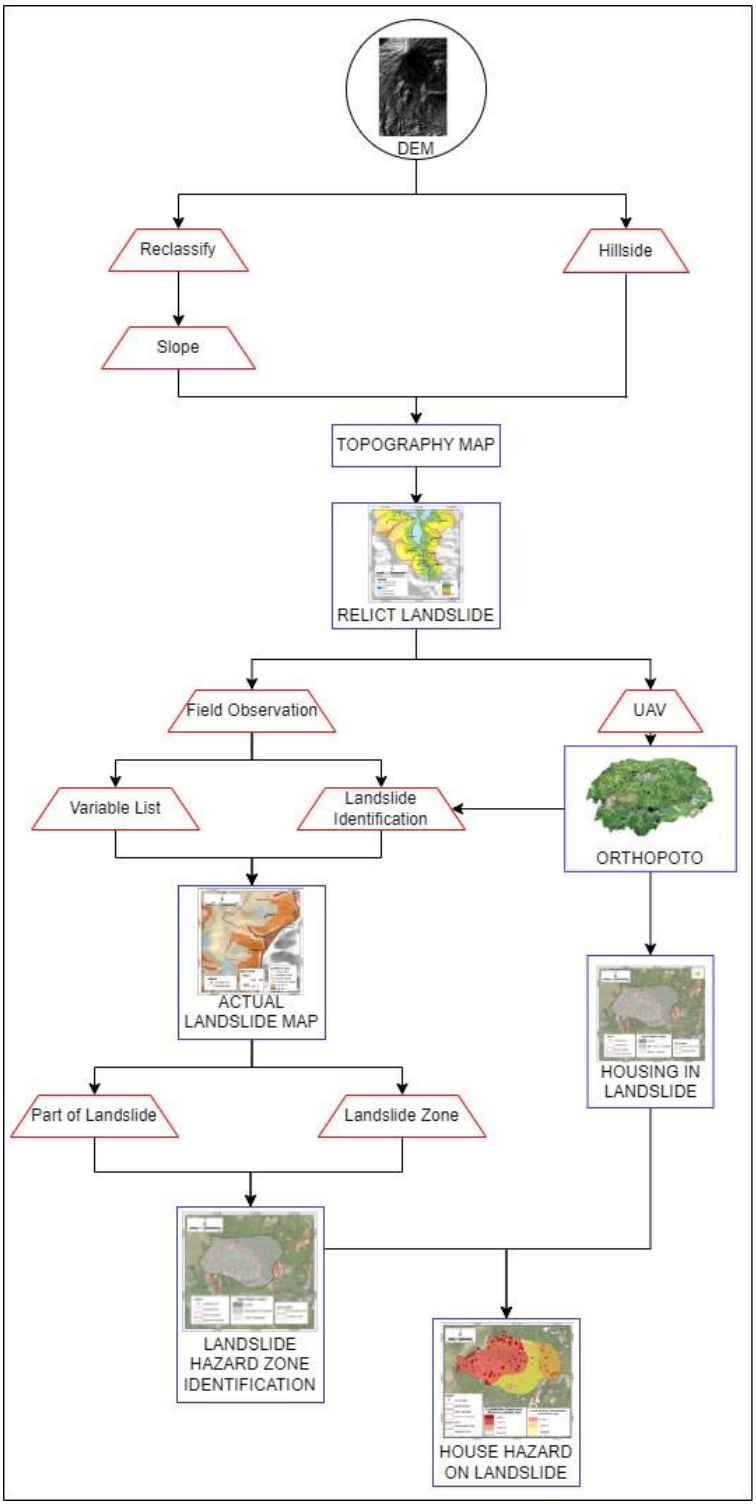

Figure 2. Research Flow Chart

RESULTS

There are 9 landslide scars in the research location using DEM (Figure 3). This result is based on the basin interpretation of height difference generated from DEM analysis with reclassify, slope, and hillside methods. Identification of landslide scars is the basis for determining the research object. Additional data from a rapid field survey and interviews with the surrounding community finally selected landslides 1 and 2 as the object of the study.

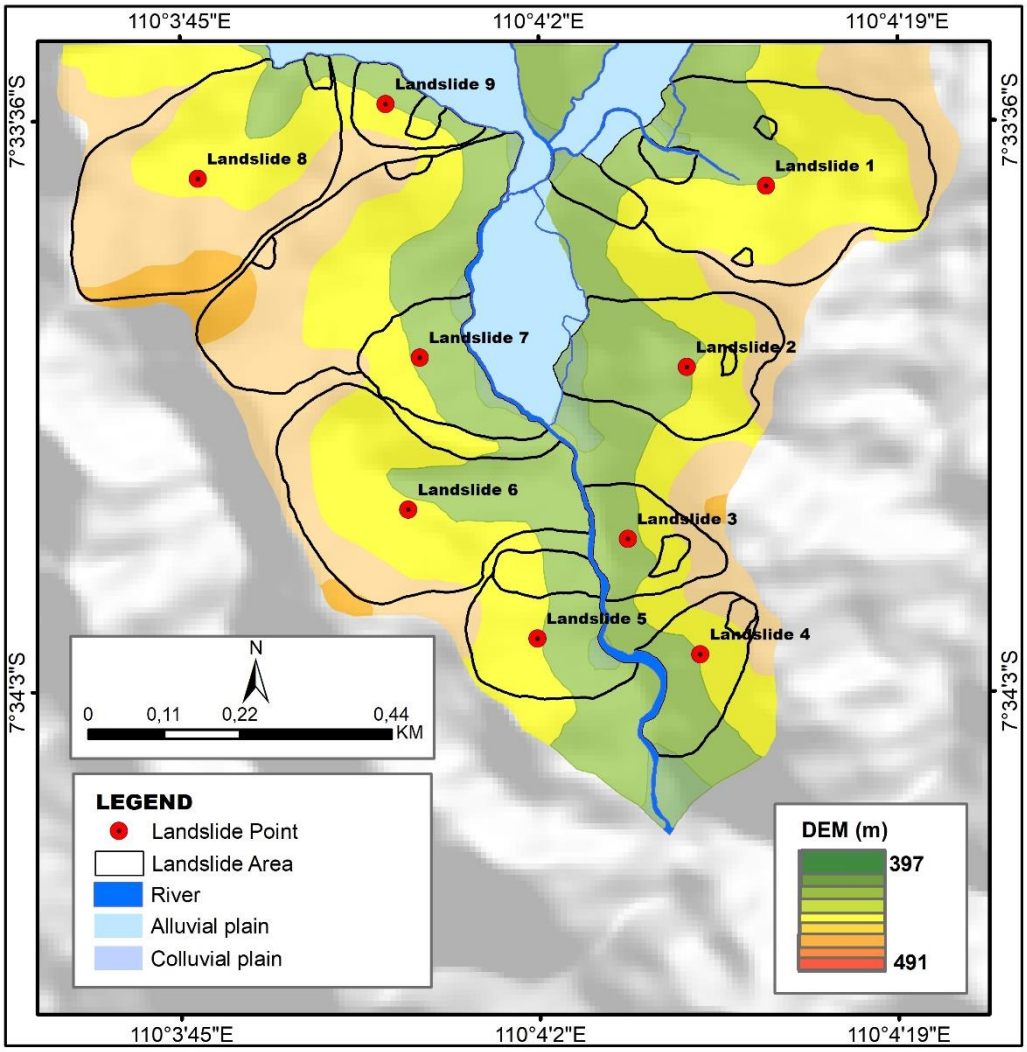

Figure 3. Landslide Identification of DEM Map

UAV Photography was conducted on landslides 1 and 2 to identify the actual boundary and analyze the new ground movement. Meanwhile, the UAV Orthophoto was processed into DEM and DSM with higher accuracy. DEM and DSM can be analyzed clearly and represented in an actual map of landslides 1 and 2. Based on the boundary, the area of landslides 1 and 2 are 11,14 Ha and 5,05 Ha, as presented in Figure 4.

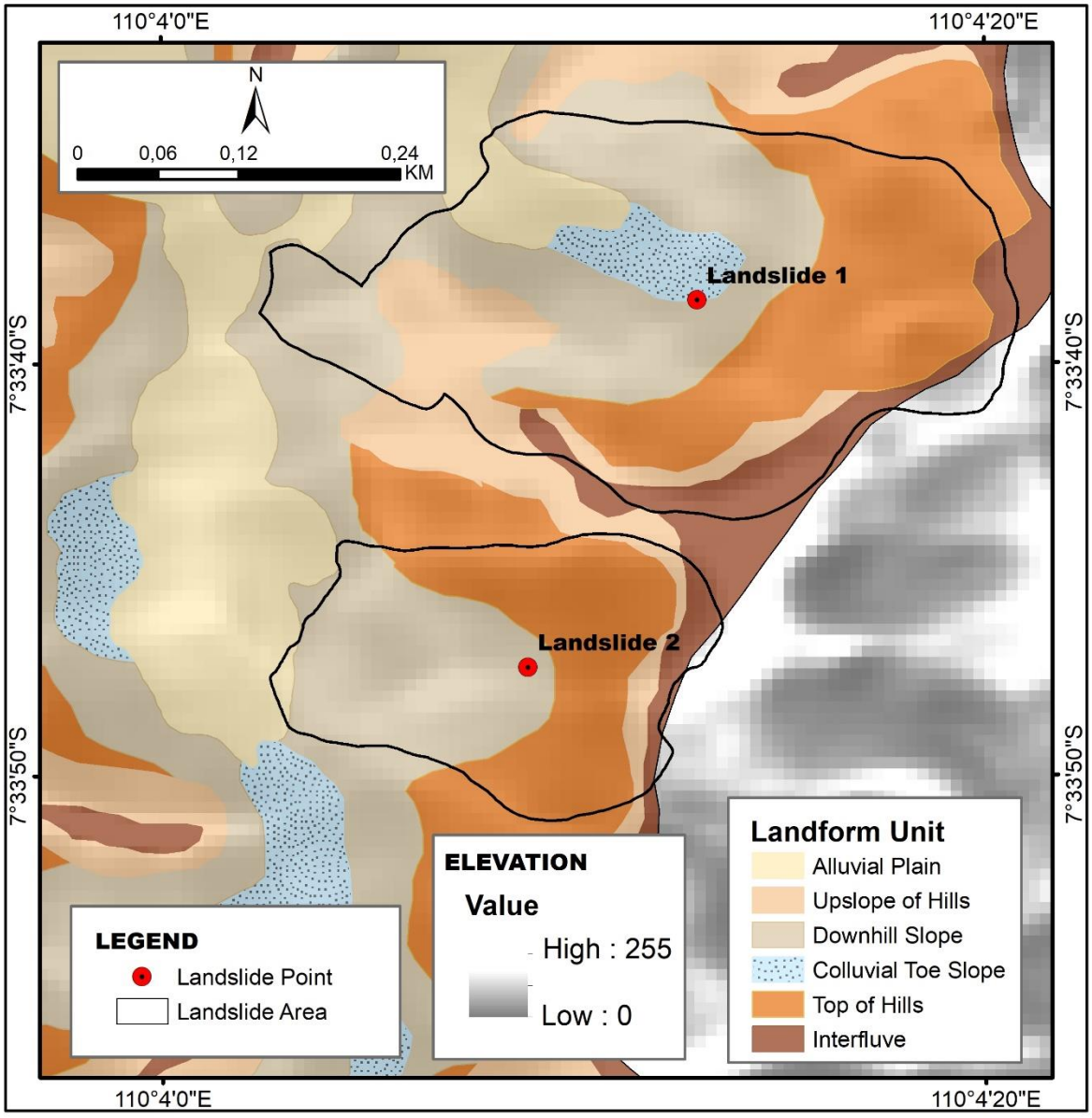

Figure 4. Actual Map of Landslides 1 and 2

The actual Map shows 4 (four) new ground movements in the area. In landslide 2, there is no new ground movement and an orthophoto is used to identify houses. Meanwhile, there are

50 and 75 residential houses scattered in landslides 1 and 2 areas. Figure 5 shows the map image of the distribution of residential houses.

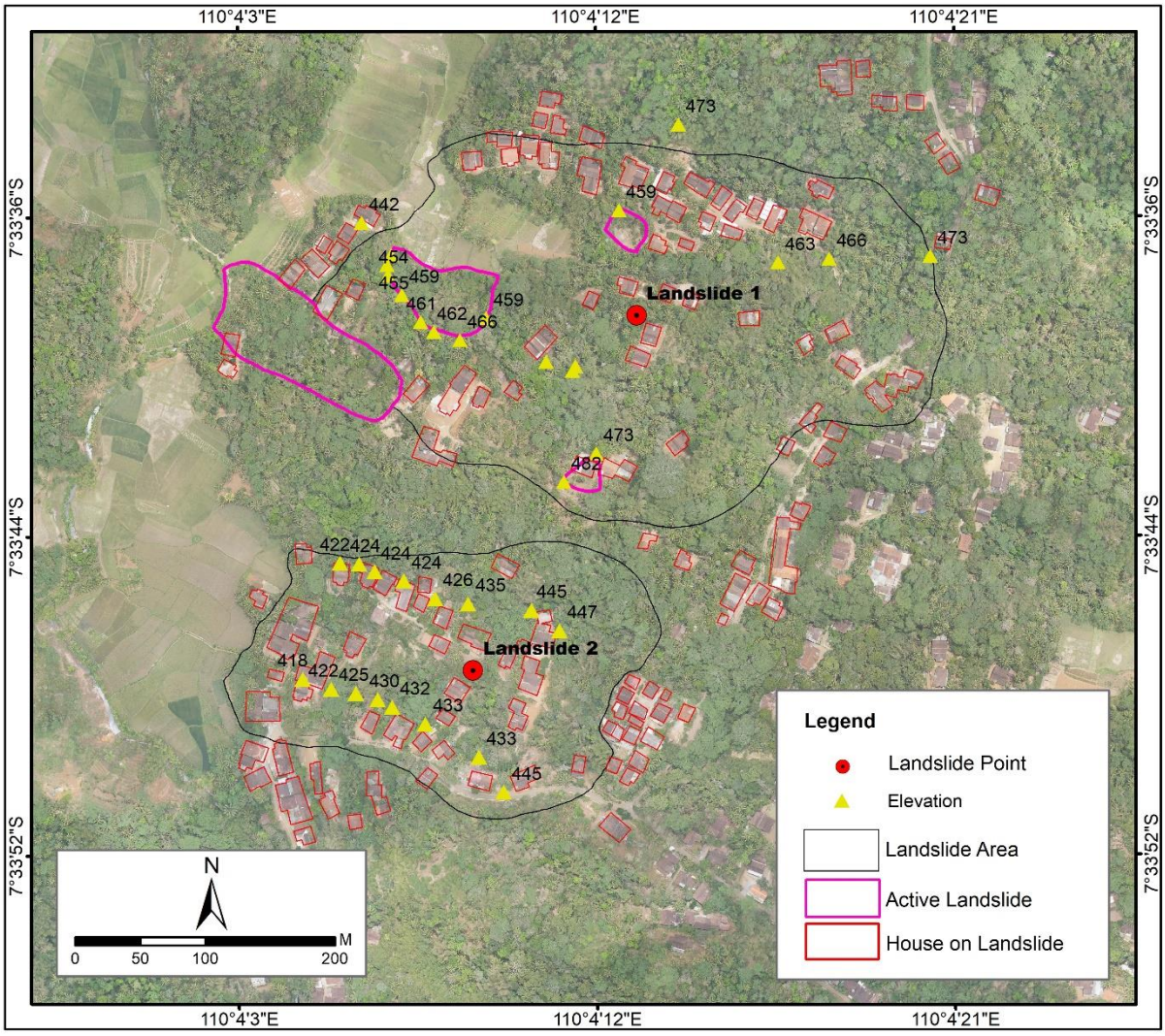

Figure 5. Distribution Map of Landslide 1 and Landslide 2 Houses

The results of the field survey and DEM from orthophoto are used to determine landslide parts, as shown in Figure 6 and Figure 7. Landslide parts are represented in 2D and 3D maps using contour data obtained from morphometric survey.

Table 2. Parts of landslides 1 and 2 based on Morphometric and Morphodynamic Data

Landslide	Elevation (meters above sea level)	Slope (^{0})	Morphodynamic	Parts of Landslide
Landslide 1	473	1	-	Crown
	473	33	Rill erosion	Scarp
	466	12	Fractures Gully	Main Body
	459	17	New Landslide (smaller size than the previous landslide) Fractures Gully Springs	Foot
Landslide 2	460	3	-	Crown
	447	8	Gully	Main Body
	422	4	Gully	Foot

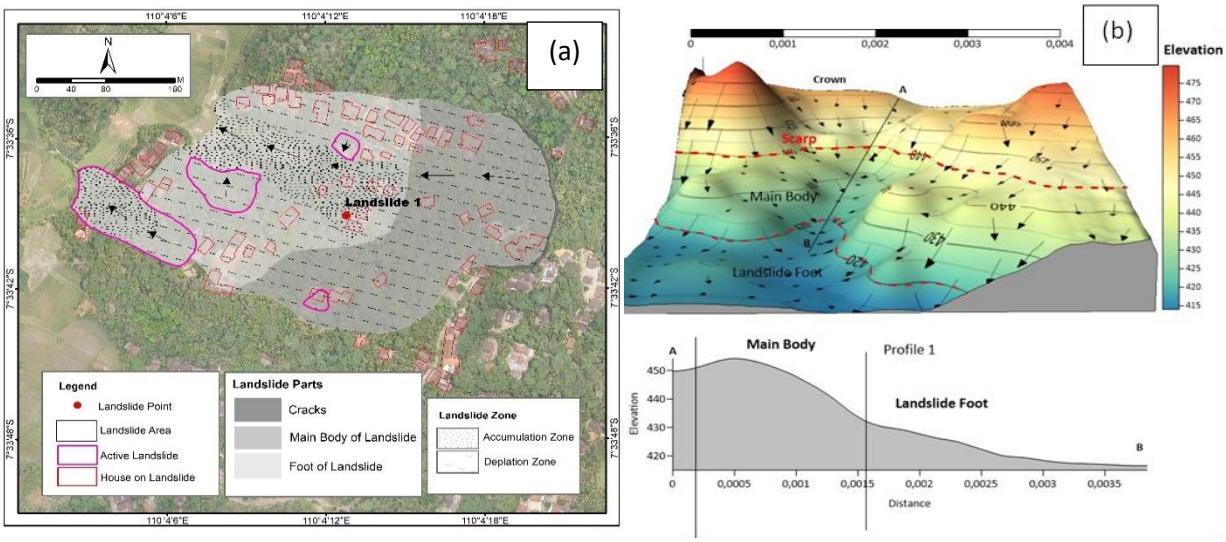

Figure 6 (a). 2D map of landslide 1, (b). 3D map of landslide 1

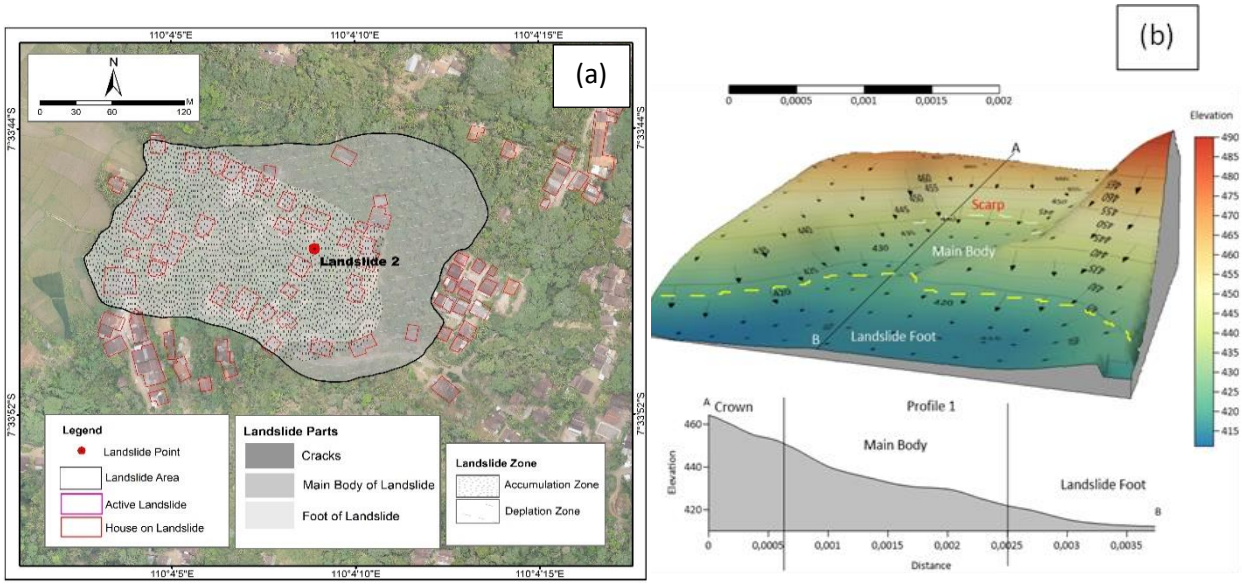

Figure 7 (a). 2D map of Landslide 2, (b). 3D Map of Landslide 2

Landslides 1 and 2 areas have different conditions based on the cross-section. The pile of material in landslide area 1 is mostly dominant in the main body and has not completely fallen to the foot. The cross-section of landslide 2 area shows that the slope moves down from the crown to the foot. The sloping condition of landslide 2 shows that landslide material has fallen to the foot. The materials in landslide 1 caused the main body of landslide 2 to be thicker and looser. Figure 8 shows the map of potential hazard zone of landslides 1 and 2.

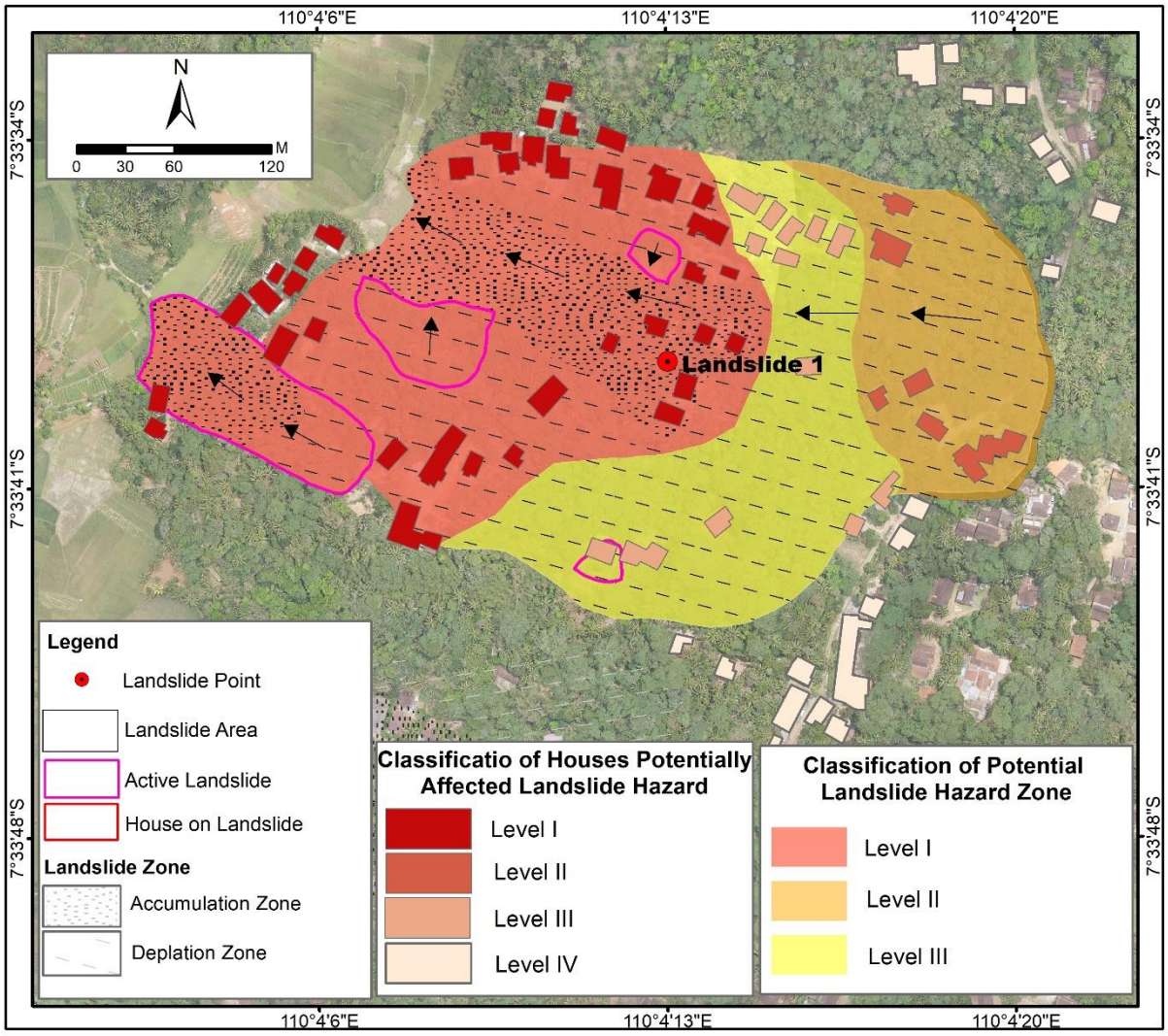

Figure 8. Map of Landslide Risk Zone 1 and Risk of Houses in Landslide 1

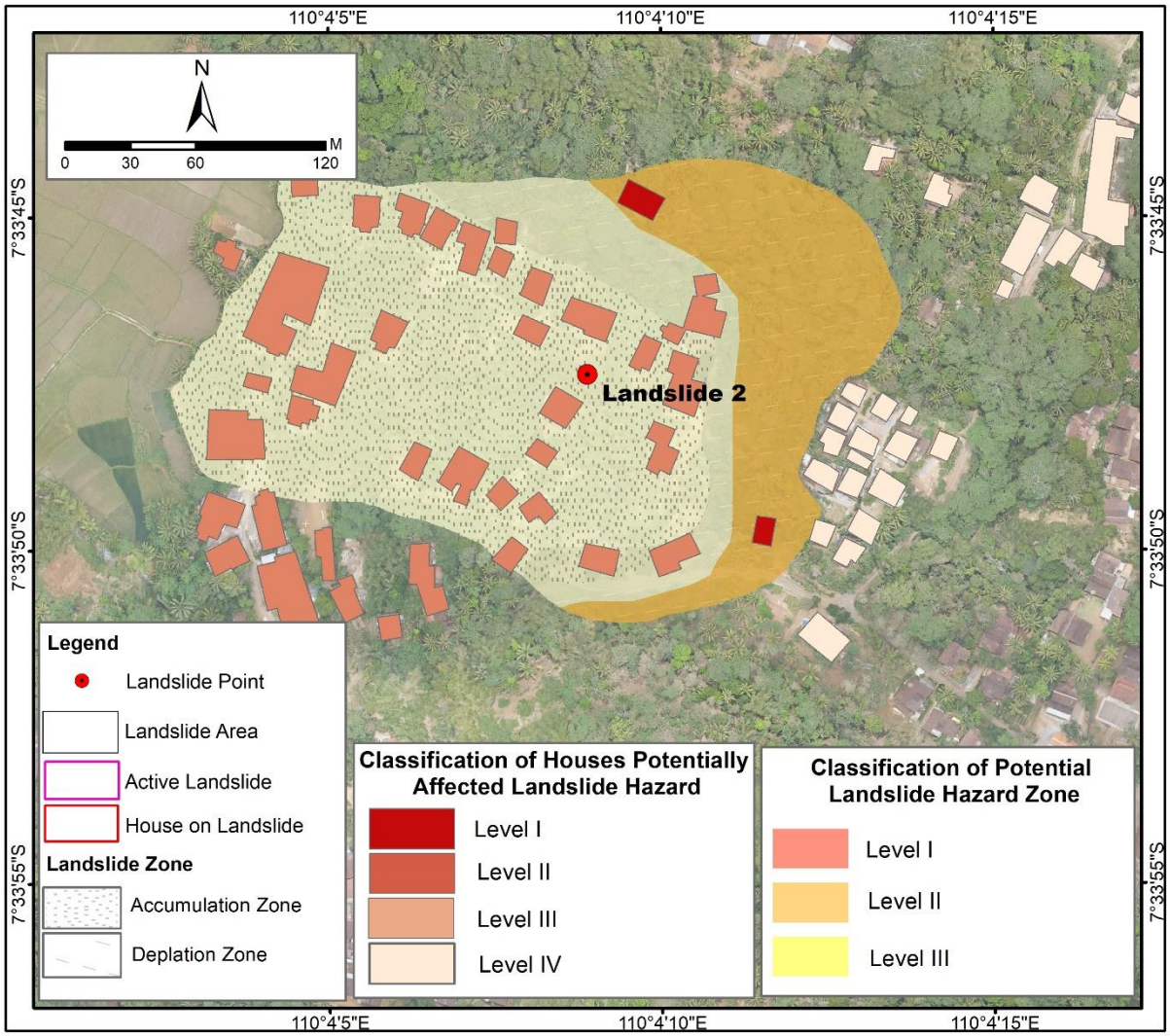

Figure 9. Map of Landslide Risk Zone 2 and Risk of Houses in Landslide 2

DISCUSSION

The description of landslide parts has been elaborated and classified by Cooper (2007). Each landslide consists of 20 parts divided into crown, main scarp, top, head, minor scarp, main body, foot, toe, tip, surface of rupture, surface of separation, displaced material, zone of depletion, zone of accumulation, depletion, depletion mass, accumulation, flank, and original ground surface. However, landslides 1 and 2 do not contain all parts. The incomplete landslide process, as well as morphodyanamic and human activities lead to the normal shape (Table 2). Landslide parts of the two areas are different, as reported by He et al. (2024) where the cutting slope changes the slope gradient. According to Nikolakopoulus et al. (2023), mass movement and erosion of the body caused reactive landslide. This result also contributes to identification of hazard zones at relict landslide and scale. The data analysis and field observations show that the scarp is part of landslide with the most potential (Tiwari et al., 2018), sequentially starting from the crown and main body (Amin et al., 2022). This is because the scarp has a steep slope and open soil conditions with low stability (Ichsandya et al. 2022) The slope becomes the benchmark for determining hazard zone in landslide area (Dotta et al., 2023). However, this condition does not occur in landslides 1 and 2. Since the slope of the scarp at landslide 1 is 33° with an interval elevation of 7 m, the area is not potential hazard (Figure 10).

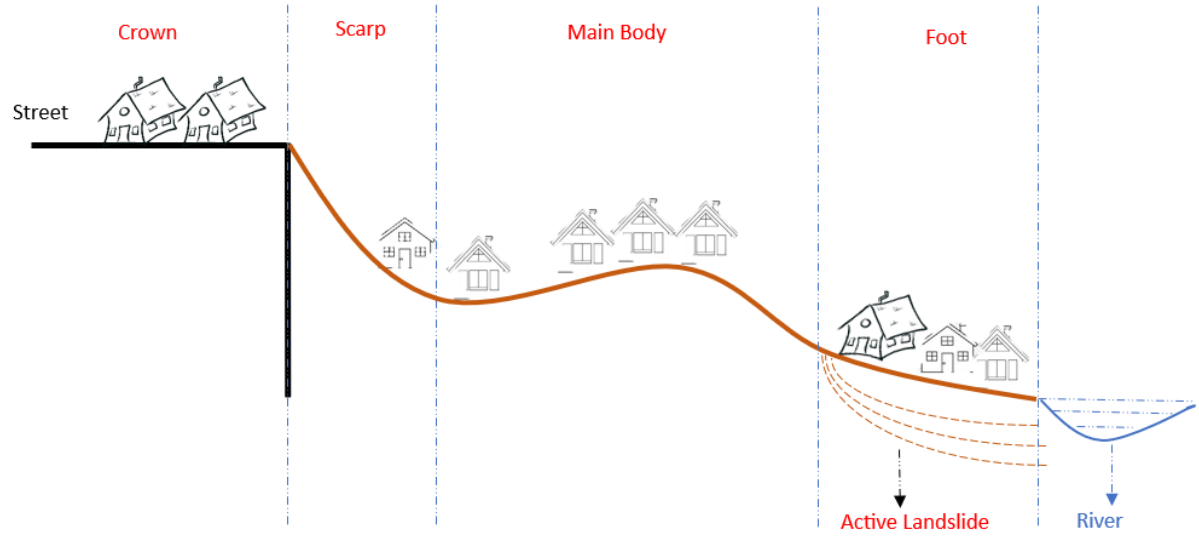

Figure 10. Landslide Hazard Risk Concept on Landslide Sections

According to orthophoto analysis, DEM, and field observation in landslide 1, potential hazard was discovered in the main body until the foot (Šilhán, 2021). In landslide 2 area, the highest potential is at the foot and the difference shows the accumulation and depletion zones considered in determining the risk.

The feature element from the perspective of geomorphology is the soil (material) of the main body (Van Tien et al., 2023). The accumulation of material that has not completely collapsed to the foot of the slope increases the size. The accumulation and large slope angle caused the main body to be unstable (He et al., 2023). However, field observations and previous research by Ramlah et al. (2020) in the Bompon watershed showed that the material accumulation is going to fall due to triggering factors. The formation of a gully causes the movement of different materials from the main body. This is an indication of slope stability since material and morphodynamic affects landslide activity in determining potential hazard zones.

Volume is an important parameter for determining hazard of landslide-affected houses (Li et al., 2020). Meanwhile, Faris et. al. (2023) analyzed landslide-affected houses based on the distance of the crown from the depletion and accumulation zones. In this study, the determinant is based on the position of houses in each part of landslide previously determined as potential level (Figure 9). Potential hazard of houses in relict areas are based on the distance from the scarp which is the most dangerous part (Tiwari et al., 2018).

CONCLUSION

In conclusion, a total of 9 relict landslides were identified at the research location. The results of DEM, DSM, and UAV photographing showed that landslides 1 and 2 had 4 and 0 cases, respectively. According to the orthophoto, there were 125 residential houses, comprising 75 and 50 in landslides 1 and 2 areas, respectively. These houses had an enormous potential hazard following the occurrence of a new landslide. In landslide 1, there was a former scar from the previous process observed directly in the field, and from the cross-section of the pile of materials. This area was dominantly in the main body of landslide and did not completely fall to the foot. In landslide 2, there was a gentle slope from the crown to the foot as reported by the condition. According to morphometric survey, orthophoto analysis, DEM, and field observation in landslide 1, the most at-potential hazard part was the main body and foot. In landslide 2, the highest potential hazard part was at the foot. The difference showed that the accumulation and depletion zones were considered in determining potential hazard. Meanwhile, the accumulation of

landslide material caused the size of the main body to be larger and unstable. In landslide 1, the highest potential hazard of houses was at the foot, while the body and crown had the greatest impact in landslide 2.

ACKNOWLEDGMENTS

Spesial thanks to Margoyo and Kajoran Society for participation in all studies conducted in the sub-district, especially in the landslide study. Appreciate to Transbulent, a natural laboratory, for accommodating and supporting all the research on the Bompon watershed. Gratefully acknowledge the Institute Teknologi PLN for supporting research enhancement.

DECLARATIONS

Conflict of Interest

We declare no conflict of interest, financial or otherwise.

Ethical Approval

On behalf of all authors, the corresponding author states that the paper satisfies Ethical Standards conditions, no human participants, or animals are involved in the research.

Informed Consent

On behalf of all authors, the corresponding author states that no human participants are involved in the research and, therefore, informed consent is not required by them.

DATA AVAILABILITY

Data used to support the findings of this study are available from the corresponding author upon request.

REFERENCES

Akcay, O. (2015). Landslide fissure inference assessment by ANFIS and logistic regression using UAS-based photogrammetry. *ISPRS International Journal of Geo-Information, 4*(4), 2131-2158. https://doi.org/10.3390/ijgi4042131

Alvioli, M., Mondini, A. C., Fiorucci, F., Cardinali, M., & Marchesini, I. (2018). Topography-driven satellite imagery analysis for landslide mapping. *Geomatics, Natural Hazards and Risk*, 9(1), 544-567. https://doi.org/10.1080/19475705.2018.1458050

Amatya, P., Kirschbaum, D., Stanley, T., & Tanyas, H. (2021). Landslide mapping using object-based image analysis and open source tools. *Engineering geology, 282*, 106000. https://doi.org/10.1016/j.enggeo.2021.10600

Amin, M. N., Umair Ashfaq, M., Mujtaba, H., Ehsan, S., Khan, K., & Faraz, M. I. (2022). Computer-aided slope stability analysis of a landslide—A Case Study of Jhika Gali Landslide in Pakistan. *Sustainability, 14*(20), 12954. https://doi.org/10.3390/su142012954

Azmoon, B., Biniyaz, A., & Liu, Z. (2022). Use of high-resolution multi-temporal DEM data for landslide detection. *Geosciences, 12*(10), 378. https://doi.org/10.3390/geosciences12100378

Cooper. R. G. (2007). *Mass movements in Great Britain*. Geological Conservation Review Series, No 33. https://www.cabidigitallibrary.org/doi/full/10.5555/20083115061

D'Ippolito, A., Lupiano, V., Rago, V., Terranova, O. G., & Iovine, G. (2023). Triggering of rain-induced landslides, with applications in southern Italy. *Water, 15*(2), 277. https://doi.or/10.3390/w15020277

de Souza, I. R., Teixeira, D. L. S., Rosa, M. B., da Silva, L. T., Ometto, J. P. H. B., Bargos, D. C., ... & Bazzan, T. (2023). Investigation of landslide hazard areas in the municipality of Cunha (Brazil) and climate projections from 2024 to 2040. *Urban Climate, 52*, 101710.https://doi.org/10.1016/j.uclim.2023.101710

Del Soldato, M., Bianchini, S., Calcaterra, D., De Vita, P., Martire, D. D., Tomás, R., & Casagli, N. (2017). A new approach for landslide-induced damage assessment. *Geomatics, Natural Hazards and Risk, 8*(2), 1524-1537. https://doi.org/10.1080/19475705.2017.1347896

Dotta, G., Fornaciai, A., Bertolini, G., Isola, I., Nannipieri, L., Favalli, M., ... & Casagli, N. (2023). Geomorphology of the upper sector of the Roncovetro active landslide (Emilia-Romagna Region, Italy). *Journal of Maps, 19*(1), 1-11. https://doi.org/10.1080/17445647.2023.2277898

Fariz, T. R., Jatmiko, R. H., & Mei, E. T. W. (2023). Pemanfaatan foto udara UAV untuk pemetaan kerentanan fisik rumah terhadap longsor di Sub-DAS Bompon. *Jurnal Ilmu Lingkungan, 21*(4), 819-829. https://doi.org/10.14710/jil.21.4.819-829

Feng, W., Tang, Y., & Hong, B. (2022). Landslide hazard assessment methods along fault zones based on multiple working conditions: A Case Study of the Lixian–Luojiabu Fault Zone in Gansu Province (China). *Sustainability, 14*(13), 8098. https://doi.org/10.3390/su14138098

Garnica-Peña, R. J., & Alcántara-Ayala, I. (2021). The use of UAVs for landslide disaster risk research and disaster risk management: A literature review. *Journal of Mountain Science, 18*(2), 482-498. https://10.1007/s11629-020-6467-7

Ghorbanzadeh, O., Didehban, K., Rasouli, H., Kamran, K. V., Feizizadeh, B., & Blaschke, T. (2020). An application of Sentinel-1, Sentinel-2, and GNSS data for landslide susceptibility mapping. *ISPRS International Journal of Geo-Information, 9*(10), 561. https://doi.org/10.339/ijgi9100561

Gutiérrez-Martín, A., Millán-Martín, J. P., Castedo, R., & Yenes, J. I. (2021). Calculation of micropiles and anchors to reinforce a slope in emergency situations: application in Málaga, Spain. Geomatics, *Natural Hazards and Risk, 12*(1), 716-740. https://doi.org/10.1080/19475705.2021.1887373

He, H., Dong, X., Du, S., Guo, H., Yan, Y., & Chen, G. (2024). Study on the stability of cut slopes caused by rural housing construction in red bed areas: a case study of Wanyuan City, China. *Sustainability, 16*(3), 1344. https://doi.org/10.3390/su16031344

He, Y., Wang, W., Zhang, L., Chen, Y., Chen, Y., Chen, B., ... & Zhao, Z. (2023). An identification method of potential landslide zones using InSAR data and landslide susceptibility. *Geomatics, Natural Hazards and Risk, 14*(1), 2185120. https://doi.org/10.1080/19475705.2023.2185120

Huang, G., Du, S., & Wang, D. (2023). GNSS techniques for real-time monitoring of landslides: A review. *Satellite Navigation, 4*(1), 5. https://doi.org/10.1186/s43020-023-00095-5

Ichsandya, D. B., Dimyati, M., Shidiq, I. P. A., Zulkarnain, F., Rahatiningtyas, N. S., Syamsuddin, R. P., & Zein, F. M. (2022). Landslide assessment using interferometric synthetic aperture radar in Pacitan, East Java. *International Journal of Electrical and Computer Engineering, 12*(3), 2614-2625. http://doi.org/10.11591/ijece.v12i3.pp2614-2625

Jacobs, L., Dewitte, O., Poesen, J., Maes, J., Mertens, K., Sekajugo, J., & Kervyn, M. (2017). Landslide characteristics and spatial distribution in the Rwenzori Mountains, Uganda. *Journal of African Earth Sciences, 134*, 917-930. https://doi.org/10.1016/j.jafrearsci.2016.05.013

Kamal, A. M., Hossain, F., Ahmed, B., Rahman, M. Z., & Sammonds, P. (2023). Assessing the effectiveness of landslide slope stability by analysing structural mitigation measures and community risk perception. *Natural Hazards, 117*(3), 2393-2418. https://doi.or/10.1007/s11069-023-05947-6

Kinde, M., Getahun, E., & Jothimani, M. (2024). Geotechnical and slope stability analysis in the landslide-prone area: A case study in Sawla–Laska road sector, Southern Ethiopia. *Scientific African, 23,* e02071. https://doi.org/10.1016/j.sciaf.2024.e02071

Kyriou, A., Nikolakopoulos, K. G., & Koukouvelas, I. K. (2022). Timely and low-cost remote sensing practices for the assessment of landslide activity in the service of hazard management. *Remote Sensing, 14*(19), 4745. https://doi.org/10.3390/rs14194745

Li, H. B., Xu, Y. R., Zhou, J. W., Wang, X. K., Yamagishi, H., & Dou, J. (2020). Preliminary analyses of a catastrophic landslide occurred on July 23, 2019, in Guizhou Province, China. *Landslides 17*, 719–724 (2020). https://doi.org/10.1007/s10346-019-01334-0

Li, L., Lan, H., & Strom, A. (2020). Automatic generation of landslide profile for complementing landslide inventory. *Geomatics, Natural Hazards and Risk, 11*(1), 1000-1030. https://doi.org/10.1080/19475705.2020.1766578

Nanehkaran, Y. A., Chen, B., Cemiloglu, A., Chen, J., Anwar, S., Azarafza, M., & Derakhshani, R. (2023). Riverside landslide susceptibility overview: leveraging artificial neural networks and machine learning in accordance with the United Nations (UN) sustainable development goals. *Water, 15*(15), 2707. https://doi.org/10.3390/w15152707

Nefros, C., Alatza, S., Loupasakis, C., & Kontoes, C. (2023). Persistent scatterer interferometry (PSI) technique for the identification and monitoring of critical landslide areas in a regional and mountainous road network. *Remote Sensing, 15*(6), 1550. https://doi.org/10.3390/rs15061550

Nefros, C., Tsagkas, D. S., Kitsara, G., Loupasakis, C., & Giannakopoulos, C. (2023). Landslide Susceptibility Mapping under the Climate Change Impact in the Chania Regional Unit, West Crete, Greece. *Land, 12*(1), 154. https://doi.org/10.3390/land12010154

Nikolakopoulos, K. G., Kyriou, A., Koukouvelas, I. K., Tomaras, N., & Lyros, E. (2023). UAV, GNSS, and InSAR data analyses for landslide monitoring in a mountainous village in western Greece. *Remote Sensing, 15*(11), 2870. https://doi.org/10.3390/rs15112870

Ogita, S., Sagara, W., & Higaki, D. (2017). *Shapes and Mechanisms of Large-Scale Landslides in Japan: Forecasting Analysis from an Inventory* (WCoE 2014–2017). In Advancing Culture of Living with Landslides: Volume 1 ISDR-ICL Sendai Partnerships 2015-2025 (pp. 315-324). Springer International Publishing. https://doi.org/10.1007/978-3-319-59469-9_26

Oliva-González, A. O., Ruiz-Pozo, A. F., Gallardo-Amaya, R. J., & Jaramillo, H. Y. (2019). Landslide risk assessment in slopes and hillsides. Methodology and application in a real case. *Dyna, 86*(208), 143-152.

Pellicani, R., Argentiero, I., & Spilotro, G. (2017). GIS-based predictive models for regional-scale landslide susceptibility assessment and risk mapping along road corridors. *Geomatics, Natural Hazards and Risk, 8*(2), 1012-1033. http://dx.doi.org/10.1080/19475705.2020.1713233

Psomiadis, E., Charizopoulos, N., Efthimiou, N., Soulis, K. X., & Charalampopoulos, I. (2020). Earth observation and GIS-based analysis for landslide susceptibility and risk assessment. *ISPRS International Journal of Geo-Information, 9*(9), 552. https://doi.org/10.3390/ijgi9090552

Ramlah, R., Hadmoko, D. S., & Setiawan, M. A. (2020). Penilaian Tingkat Aktivitas Longsor di Sub-DAS Bompon. *Media Komunikasi Geografi, 21*(1), 12-26. https://doi.org/10.23887/mkg.v20i2.21360

Rong, G., Li, K., Han, L., Alu, S., Zhang, J., & Zhang, Y. (2020). Hazard mapping of the rainfall–landslides disaster Chain based on GeoDetector and Bayesian Network Models in Shuicheng County, China. *Water, 12*(9), 2572. https://doi.org/10.3390/w12092572

Saenkang, P., & Setiawan, H. (2022). Landslide susceptibility zone in steep slope landscape at Gunung Kidul Regency, southeast part of Yogyakarta, Indonesia. In *IOP Conference Series: Earth and Environmental Science*, *1071*(1). https://doi.org/10.1088/1755-1315/1071/1/012002

Setyowati, D. L. (2019). *Pendidikan Kebencanaan*. Universitas Negeri Semarang.

Shan, Y., Xu, Z., Zhou, S., Lu, H., Yu, W., Li, Z., ... & Li, W. (2023). Landslide hazard assessment combined with InSAR Deformation: A Case Study in the Zagunao River Basin, Sichuan Province, Southwestern China. *Remote Sensing, 16*(1), 99. https://doi.org/10.3390/rs16010099

Shano, L., Raghuvanshi, T. K., & Meten, M. (2020). Landslide susceptibility evaluation and hazard zonation techniques–a review. *Geoenvironmental Disasters, 7*, 1-19. https://doi.org/10.1186/s40677-020-00152-0

Shi, K., Yu, B., Ma, J., Cao, W., & Cui, Y. (2023). Impacts of slope climbing of urban expansion on global sustainable development. *The Innovation, 4*(6). https://doi.org/10.1016/j.xinn.2023.100529

Šilhán, K. (2021). A new tree-ring-based index for the expression of spatial landslide activity and the assessment of landslide hazards. *Geomatics, Natural Hazards and Risk, 12*(1), 3409-3428. https://doi.org/10.1080/19475705.2021.20111790

Sun, J., Yuan, G., Song, L., & Zhang, H. (2024). Unmanned Aerial Vehicles (UAVs) in landslide investigation and monitoring: A Review. *Drones, 8*(1), 30. https://doi.org/10.3390/drones8010033

Thomas, J., Gupta, M., Srivastava, P. K., & Petropoulos, G. P. (2023). Assessment of a dynamic physically based slope stability model to evaluate timing and distribution of rainfall-induced shallow landslides. *ISPRS International Journal of Geo-Information, 12*(3), 105. https://doi.org/10.3390/10.3390/ijgi12030105

Tiwari, A., Narayan, A. B., Dwivedi, R., Dikshit, O., & Nagarajan, B. (2020). Monitoring of landslide activity at the Sirobagarh landslide, Uttarakhand, India, using LiDAR, SAR interferometry and geodetic surveys. *Geocarto International, 35*(5), 535-558. https://doi.org/10.1080/10106049.2018.1524516

Triatmadja, R. (2011). *Tsunami: Kejadian, Penjalaran, Daya Rusak, Dan Mitigasinya*. Gadjah Mada University Press

Van Tien, D., Thanh, N. K., Quang, L. H., Ha, D. N., Sassa, K., Miyagi, T., & Abe, S. (2023). *Landslide risk assessment in the tropical zone of Vietnam as a contribution to the mitigation of natural disaster vulnerability*. In Progress in Landslide Research and Technology, 2(1), 275-305. Cham: Springer Nature Switzerland.

Wang, P., Liu, H., Nie, G., Yang, Z., Wu, J., Qian, C., & Shu, B. (2022). Performance evaluation of a real-time high-precision landslide displacement detection algorithm based on GNSS virtual reference station technology. *Measurement, 199*, 111457. https://doi.org/10.1016/j.measurement.2022.11457

Xi, R., Jiang, W., Xuan, W., Xu, D., Yang, J., He, L., & Ma, J. (2023). Performance Assessment of Structural Monitoring of a Dedicated High-Speed Railway Bridge Using a Moving-Base RTK-GNSS Method. *Remote Sensing, 15*(12), 3132. https://doi.org/10.3390/rs1523132

Yan, T., Xiong, J., Ye, L., Gao, J., & Xu, H. (2023). Field investigation and finite element analysis of landslide-triggering factors of a cut slope composed of granite residual soil: A case study of Chongtou Town, Lishui City, China. *Sustainability, 15*(8), 6999. https://doi.org/10.3390/su15086999

Zhang, S., Li, C., Peng, J., Lv, Y., Wang, S., Peng, D., ... & Ouyang, C. (2024). Physical vulnerability assessment of damaged buildings to the Shenzhen catastrophic CSW landslide. *Landslides,* 1-17. https://doi.org/10.1007/s10346-023-02200-w